ARTICLES ON NEAR-FIELD MICROSCOPY AND SPECTROSCOPY

Probing single molecule orientations in model lipid membranes with near-field scanning optical microscopy

Christopher W. Hollars and Robert C. Dunn[a)]
Department of Chemistry, University of Kansas, Lawrence, Kansas 66045

(Received 18 October 1999; accepted 1 February 2000)

Single molecule near-field fluorescence measurements are utilized to characterize the molecular level structure in Langmuir–Blodgett monolayers of *L*-α-dipalmitoylphosphatidylcholine (DPPC). Monolayers incorporating 3×10^{-4} mol % of the fluorescent lipid analog *N*-(6-tetramethylrhodaminethiocarbamoyl)-1,2-dihexadecanoyl-*sn*-glycero-3-phosphoethanolamine, triethylammonium salt (TRITC–DHPE) are transferred onto a freshly cleaved mica surface at low ($\pi=8$ mN/m) and high ($\pi=30$ mN/m) surface pressures. The near-field fluorescence images exhibit shapes in the single molecule images that are indicative of the lipid analog probe orientation within the films. Modeling the fluorescence patterns yields the single molecule tilt angle distribution in the monolayers which indicates that the majority of the molecules are aligned with their absorption dipole moment pointed approximately normal to the membrane plane. Histograms of the data indicate that the average orientation of the absorption dipole moment is 2.2° ($\sigma=4.8°$) in monolayers transferred at $\pi=8$ mN/m and 2.4° ($\sigma=5.0°$) for monolayers transferred at $\pi=30$ mN/m. There is no statistical difference in the mean tilt angle or distribution for the two monolayer conditions studied. The insensitivity of tilt angle to film surface pressure may arise from small chromophore doped domains of trapped liquid-expanded lipid phase remaining at high surface pressure. There is no evidence in the near-field fluorescence images for probe molecules oriented with their dipole moment aligned parallel with the membrane plane. We do, however, find a small but significant population of probe molecules (~13%) with tilt angles greater than 16°. Comparison of the simultaneously collected near-field fluorescence and force images suggests that these large angle orientations are not the result of significant defects in the films. Instead, this small population may represent a secondary insertion geometry for the probe molecule into the lipid monolayer. [S0021-9606(00)70616-7]

INTRODUCTION

Near-field scanning optical microscopy (NSOM) offers new opportunities for probing sample structure and organization at the molecular level.[1–6] For example, the single molecule fluorescence sensitivity and unique properties of the fields near the NSOM aperture have been exploited to characterize the three-dimensional orientation of individual chromophores in polymers.[7,8] Typically, measurements of molecular orientation are carried out on large ensembles where the sample is required to have a high degree of long range order.[9–14] These types of bulk measurements average across the specific distribution of individual molecules which can hide important sample details. The single molecule orientation sensitivity of NSOM combined with its high spatial resolution fluorescence and force imaging capabilities, therefore, provide a powerful new tool for many applications.

Recently, far-field techniques have also demonstrated the capability of determining molecular orientations at the single molecule level at both low[15,16] and room temperatures.[17–19] At low temperature, the orientation of terrylene molecules in a Shpol'skii matrix was characterized and at room temperature the distribution of carbocyanine derivatives in thin films of polymethylmethacrylate (PMMA) was investigated.[15–19] Both the far-field and near-field single molecule studies have illustrated the utility of measuring individual orientation distributions. In particular, the NSOM technique is unique in that these measurements are carried out with subdiffraction limit spatial resolution and yield a simultaneous force mapping of the sample topography. This combined capability affords the precise determination of single molecule orientations in regions of the sample that are physically well defined by the topography image. This is especially helpful for biological applications that often exhibit complex morphologies.[20–25]

While technically difficult due to the strict requirements on tip quality, single molecule NSOM orientation measurements offer a new perspective on sample organization. These measurements are widely applicable for samples ranging from highly ordered crystals to highly disordered polymers or glass systems. One area that seems particularly well suited

a)Author to whom correspondence should be addressed.

to take advantage of these capabilities is in the biological sciences. These semiordered systems are often characterized by domain or compartment formation within which there can be a high degree of local order. Probing the three-dimensional orientation of individual proteins in cellular membranes, for instance, may shed light on important structure-function relationships. NSOM complements the sectioning capabilities of confocal microscopy by providing high resolution measurements of only those species located near the NSOM aperture. Therefore, the collection of optical (orientation) and force (topography) information with NSOM should be especially informative for membrane bound species.

Lipid monolayers and bilayers formed using the Langmuir–Blodgett (LB) technique have long been used as models for biological membranes.[26–29] Extensive studies have characterized the phase partitioning in these films and the effects that biologically relevant additives such as cholesterol and small peptides can have on membrane properties.[30,31] Often, these effects can be observed by monitoring changes in the film structure using high resolution techniques such as fluorescence microscopy,[27,28,32] scanning probe microscopy,[33–37] or electron microscopy.[38] Recently, our group and others have illustrated the utility of NSOM for these types of measurements, which has resulted in the observation of new structures and processes at the submicron level.[31,39–44]

The capabilities of NSOM are often complimentary with other high resolution techniques. For studies on model lipid membranes, the simultaneously collected near-field fluorescence and force information provide a unique window into the phase partitioning and effects of constituents on membrane structure. This was illustrated by Hwang *et al.*, where high resolution near-field fluorescence measurements revealed new structures in lipid monolayers of *L*-α-dipalmitoylphosphatidylcholine (DPPC) doped with cholesterol and ganglioside G_{M1}.[31] Following these results, we have shown that the phase partitioning in DPPC monolayers can be unambiguously assigned by comparing the small height differences (5 to 8 Å) observed in the near-field force image with the near-field fluorescence image.[39,40,44] We also showed that for model lipid bilayers, NSOM can uniquely probe the phase partitioning on either side of the membrane with nanometric resolution.[40]

Here, we discuss an extension of these results down to the molecular level where specific measurements of probe orientation within the membrane are possible. Single molecule measurements made with NSOM on the fluorescent lipid analog *N*-(6-tetramethylrhodaminethiocarbamoyl)-1,2-dihexadecanoyl-*sn*-glycero-3-phosphoethanolamine, triethylammonium salt (TRITC–DHPE) doped into LB monolayers of DPPC are used to characterize the molecular level structure. These measurements follow the original report of Betzig and Chichester which illustrated the capability of probing the three dimensional orientation of single chromophores with NSOM.[8]

As was shown by Betzig and Chichester, unique patterns are observed in the single molecule images which can be simulated using a simplified model for the near-field aperture.[8] This model treats the diffraction of light through an infinitely thin, perfectly conducting screen and was first developed for other applications by Bethe in 1944,[45] with corrections later added by Bouwkamp in 1950.[46] These calculations predict a curvature in the electric field near the boundaries of a subwavelength aperture. The measurements of Betzig and Chichester confirmed the presence of similar fields near the NSOM aperture and illustrated how these can be utilized to probe the orientation of single fluorophores.

In this paper, we exploit these properties to examine the orientation distribution of probe molecules doped into model lipid films of DPPC. By modeling the observed near-field fluorescence patterns using Bethe–Bouwkamp theory, the single molecule tilt angles are extracted for molecules doped into DPPC monolayers at both high ($\pi = 30$ mN/m) and low ($\pi = 8$ mN/m) surface pressures. Histograms of the resulting tilt angles for the two film conditions, surprisingly leads to distributions that are statistically identical. This indicates that the immediate structure around the probe molecules in each DPPC film condition are similar, suggesting that the lipid probe remains in a similar lipid phase environment that persists even at high surface pressure. These measurements are compared with recent single molecule far-field fluorescent studies which show that the dopant molecules do sense a change in the immediate surroundings as the surface pressure is increased.[47] Together, the near-field and far-field fluorescence measurements provide a coherent view of membrane properties that are normally hidden in bulk measurements. These studies, therefore, provide a direct, nonensemble averaged window into the lipid film microstructure and homogeneity at two different surface pressures.

MATERIALS AND METHODS

Lipid monolayers were transferred onto a freshly cleaved mica surface using a computer controlled Langmuir–Blodgett trough (Model 611, Nima Technology). The trough incorporates a Wilhelmy sensor to precisely monitor the surface pressure during film compression and deposition. *L*-α-dipalmitoylphosphatidylcholine (DPPC) (Sigma) and *N*-(6-tetramethylrhodaminethiocarbamoyl)-1,2-dihexadecanoyl-*sn*-glycero-3-phosphoethanolamine, triethylammonium salt (TRITC–DHPE) (Molecular Probes) were used without further purification. DPPC was dissolved in spectral grade chloroform to provide a concentration of 1 mg/ml. A small volume of TRITC–DHPE in optima grade methanol was added to the DPPC solution to produce DPPC/3×10^{-4} mol % TRITC–DHPE mixture.

Lipid monolayers were formed by dispersing approximately 50 μL of the DPPC solution onto an 18 MΩ water subphase at room temperature. After the solvent was allowed to evaporate, the film was compressed at a rate of 100 cm^2/min to the desired surface pressure. The compressed film was held at the desired pressure for several minutes prior to transfer onto a freshly cleaved mica surface at a rate of 25 mm/min. For this study, films were transferred onto the substrate at pressures of $\pi = 8$ mN/m and $\pi = 30$ mN/m in a headgroups down orientation.

The dye containing lipid monolayers were studied with a custom-built near-field microscope.[20,48] Briefly, the NSOM

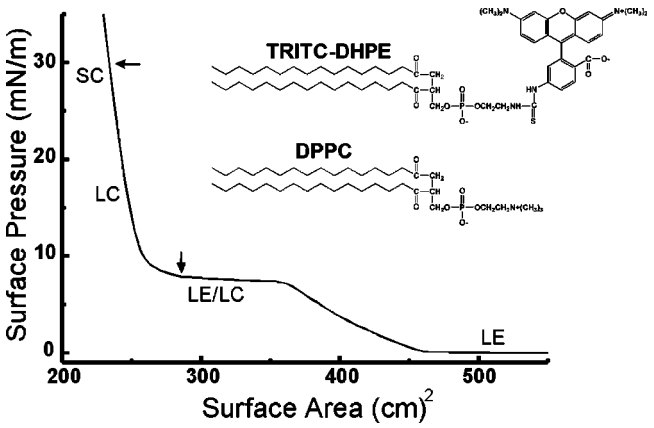

FIG. 1. Pressure isotherm for DPPC/0.25 mol % TRITC–DPHE on a 18 MΩ water subphase. The various regions along the pressure isotherm are characterized by the existing lipid phases and proceed in increasing degree of order from the liquid-expanded (LE) region, liquid-expanded/liquid-condensed (LE/LC) coexistence region, liquid-condensed (LC), and highly ordered solid-condensed (SC) regions. Arrows locate the regions of the pressure isotherm at which films were transferred onto a mica substrate. Also shown are the chemical structures for DPPC and the fluorescent probe molecule, TRITC–DPHE.

is built on an inverted fluorescence microscope (Zeiss, Axiovert 135TV) and is operated using commercially available scanning probe electronics and software (Digital Instruments, Nanoscope IIIa), with only minor modifications made for near-field microscopy. Aluminum coated near-field fiber optic probes are fabricated from 125 μm single-mode optical fiber (Newport Corp.) in either the straight geometry or cantilevered design using a micropipette puller (Sutter Instruments, P-2000) and home-built evaporation chamber.[20,49] For experiments utilizing straight near-field probes, a custom designed near-field head is utilized to implement the shear-force feedback mechanism. For cantilevered probes, a commercial AFM head (Digital Instruments, Dimension) is utilized to implement a tapping-mode feedback scheme.

In either imaging mode, the LB film is mounted directly beneath the tip on a closed loop $x-y$ piezo scanner that is used to raster scan the sample under the near-field tip. The 514 nm line of an argon ion laser (Liconix, 5000 series) is passed through a λ/2 plate and λ/4 plate to control the polarization and subsequently coupled into an optical fiber, the end of which is fashioned into a near-field tip. Light exiting the near-field tip excites fluorescence in the sample which is collected from below with a high NA oil immersion objective lens (Zeiss, Fluar 40X 1.3 NA). The residual excitation light is filtered (Chroma) and the collected fluorescence signal is imaged onto an avalanche photodiode detector (EG&G, SPCM-200).

RESULTS

Figure 1 shows a typical pressure isotherm for DPPC on a water subphase with arrows marking the locations at which films were transferred onto a freshly cleaved mica surface. At low surface pressures, in the phase coexistence region, the monolayer contains a mixture of less ordered liquid-expanded (LE) and more ordered liquid-condensed (LC) phases. As the film is compressed further, a phase transition to a highly ordered solid-condensed (SC) state is observed.[50] The inset of Fig. 1 shows the chemical structures for the DPPC lipid and the fluorescent lipid probe TRITC–DHPE.

Near-field fluorescence and tapping-mode force images are shown in Fig. 2(A) and 2(B), respectively, for a DPPC/0.25 mol % TRITC–DHPE monolayer deposited onto mica at a surface pressure of $\pi = 8$ mN/m. The LC/LE phase partitioning in the monolayer is characterized by a 5 to 8 Å height difference between the LE and more upright LC phases in the force image and bright regions in the near-field fluorescence image.[39,40,44] Comparison of the two images shows that the TRITC–DHPE probe preferentially partitions into the less ordered LE phase. The simultaneous near-field fluorescence and force images therefore provides an unambiguous view into the phase partitioning of the film. As the concentration of the fluorescent probe is reduced to DPPC/3×10^{-4} mol % TRITC–DHPE, single fluorescent molecules can be resolved in the NSOM fluorescence images. For example, Figs. 2(C) and 2(D) show near-field fluorescence and shear-force images of a typical monolayer deposited at $\pi = 8$ mN/m containing the reduced concentration of dye. The bright spots in the image represent the fluorescence from single molecules in the DPPC monolayer. Figures 2(A) and 2(B) were collected using a cantilevered NSOM probe operating in tapping-mode feedback while Figs. 2(C) and 2(D) were collected using a conventional NSOM probe operating in shear-force feedback. The shear-force image shown in Fig. 2(D) is lower in quality than the tapping-mode force image shown in Fig. 2(B), but the height changes in the monolayer are still discernible. Straight NSOM tips were utilized in this study due to their superior polarization characteristics.

Upon closer inspection of the NSOM fluorescence image shown in Fig. 2(C), many of the single molecule features are seen to actually consist of two lobes. As originally shown by Betzig and Chichester, the origin of these shapes can be understood within the context of Bethe–Bouwkamp theory for light diffracting through a subwavelength aperture.[8] These calculations treat the passage of light through a small hole in an infinitely thin, perfectly conducting screen.[45,46] Surprisingly, this simplified model provides a reasonably accurate picture of a near-field aperture, allowing for the calculation of the field distribution in and around a near-field tip. Results from such calculations are shown schematically in Fig. 3.

The predicted electric field contains z-components near the tip edges which can excite chromophores with absorption transition dipole moments pointing towards the aperture. Referring to Fig. 3, as the near-field tip is scanned across a chromophore with a z-oriented transition dipole moment, such as that shown by the double arrow, overlap is greatest near the tip edges and reduced when located directly beneath the aperture. Therefore, fluorescence is enhanced when the molecule is located at the edges of the aperture and diminished when it is located directly beneath the center of the tip. This leads to the patterns seen in the near-field fluorescence image shown in Fig. 2(C). These arguments can be used to qualitatively conclude that a significant number of the TRITC–DHPE probe molecules in the DPPC monolayer are oriented with their absorption transition dipole moment (long

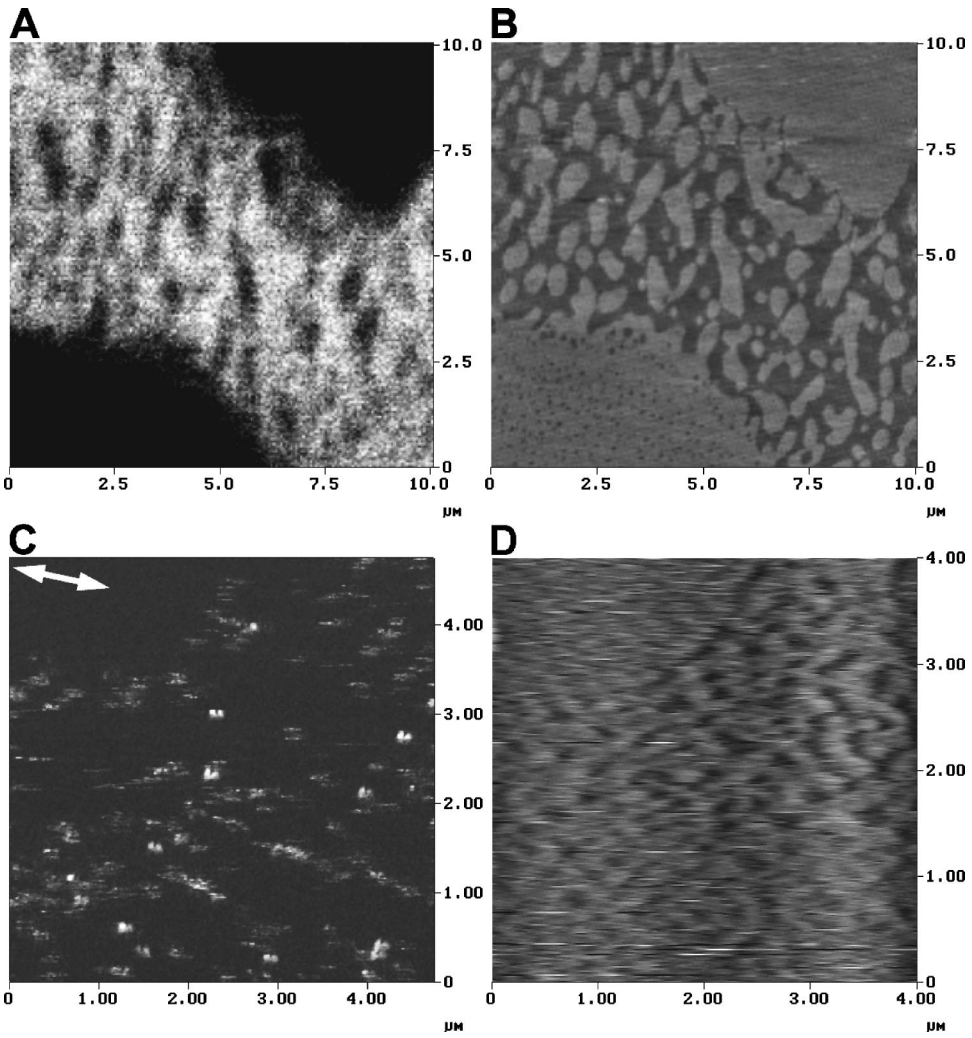

FIG. 2. (A) Near-field fluorescence and (B) tapping-mode force images of a DPPC/0.25 mol % TRITC–DPHE monolayer transferred at a surface pressure of $\pi = 8$ mN/m. Coexisting LE and LC phases in the films are characterized by low (LE) and high (LC) topography regions in the force image with a height difference of 5–8 Å. LE regions of lower topography correspond to bright areas in the near-field fluorescence image showing that TRITC–DPHE partitions into the LE phase. (C) Near-field fluorescence and (D) shear-force images of a DPPC/3×10^{-4} mol % TRITC–DPHE monolayer transferred at a surface pressure of $\pi = 8$ mN/m. The bright features in the near-field fluorescence image correspond to the fluorescence from single TRITC–DPHE probe molecules in the DPPC monolayer. The dual-lobed pattern of the molecules indicates that the absorption transition dipole moment is oriented approximately perpendicular to the plane of the membrane. The polarization of the excitation light is indicated by the double arrow in the upper left corner of (C).

axis of the chromophore) aligned in the *z* direction.

Representative examples of the near-field fluorescence patterns observed in DPPC films at both low and high surface pressures are shown in Fig. 4. All data presented have been rotated such that the excitation polarization is aligned along the horizontal direction of the images. The direction of the polarization was chosen as not to coincide with either the vertical or horizontal scan directions to avoid artifacts from emission intensity fluctuations that are inherent in single molecule studies. The progression in the asymmetry of the lobe amplitudes correlates with the degree of tilt in the probe molecule. This can be easily understood by referring back to the schematic shown in Fig. 3. For molecules with transition dipole moments aligned perfectly in the *z* direction, the overlap with the field is equivalent for both sides of the tip aperture. This leads to lobes of equal amplitude in the fluorescence image [Fig. 4(A)]. However, for molecules that are tilted [Figs. 4(B) and 4(C)], there will be a difference in the degree of overlap when the molecule is located under each side of the tip. Therefore, the distribution in lobe amplitudes shown in Fig. 4 reveal both the direction in which the transition dipole moment is tilted and the degree to which it is tilted. To provide a quantitative basis for comparison, single molecule fluorescence data such as that shown in Fig. 4 can be compared with calculated fluorescence patterns using the simplified view of the near-field aperture.

As shown in the original report by Betzig and Chichester, the single molecule patterns can be modeled by orienting a transition dipole beneath the tip and exciting it with the

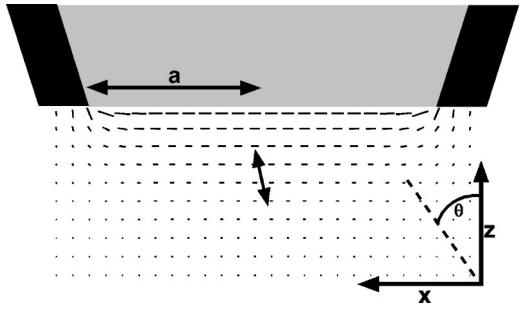

FIG. 3. Schematic representation of the near-field tip and the calculated electric field modeled using Bethe–Bouwkamp theory. The double arrow represents the absorption transition dipole moment of a probe molecule located beneath the tip. For *z*-oriented molecules such as that represented by the double arrow, significant overlap between the electric field and the transition dipole moment only occurs when the molecule is located near the edges of the tip. This leads to dual-lobed features in the single molecule fluorescence image.

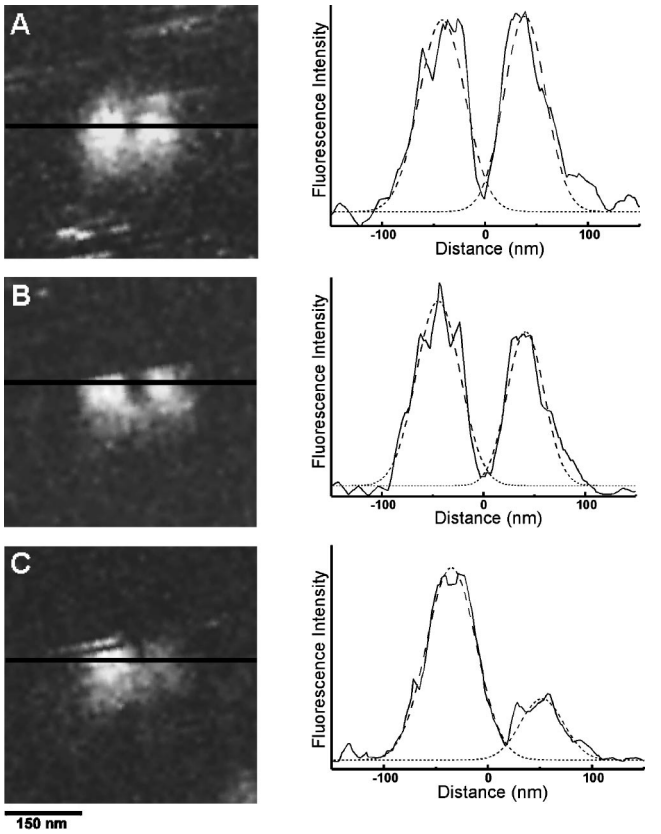

FIG. 4. Representative near-field single molecule fluorescence data extracted from images such as that shown in Fig. 2(C). The left panels show the fluorescence signal and the right panels display line-cuts through the data (solid lines). Examples have been chosen to represent a range of tilt angles present in the near-field images. The tilt of the chromophore increases down the series of images resulting in an increasing differential in the intensity from the two lobes. The line cuts are fit with a sum of Gaussians (dashed lines) to quantify the peak amplitude ratio used to determine the tilt angle. The analysis results in tilts corresponding to 0.0°, 2.1°, and 13.5° for images (A), (B), and (C), respectively. The line cuts were performed in the direction of the excitation polarization at the positions indicated by the horizontal lines inserted into the left panels. The images in the left panels have been rotated for this alignment.

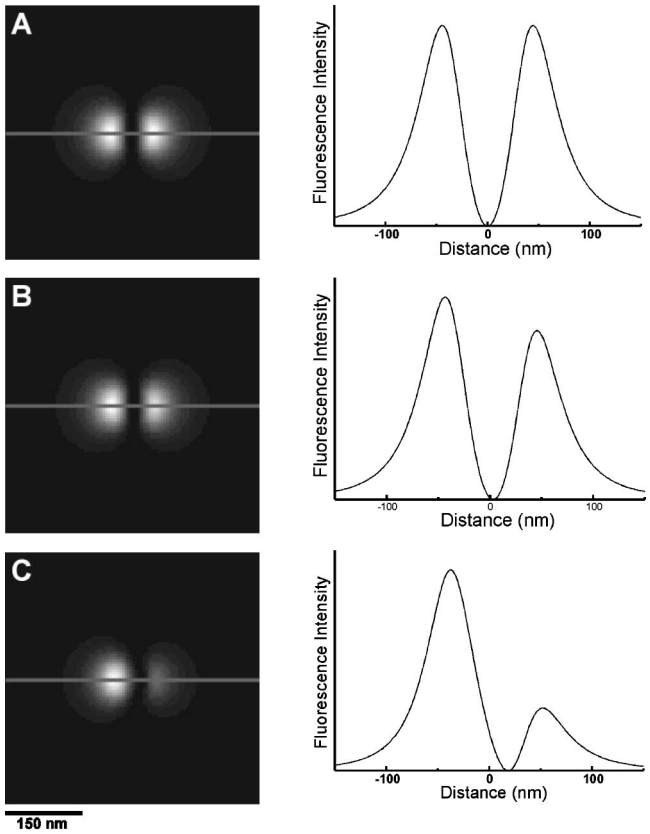

FIG. 5. Simulated fluorescence signals calculated using Bethe–Bouwkamp theory to model the near-field fluorescence patterns displayed in Fig. 4. The left panels show the simulated fluorescence signal and the right panels display line cuts through the intensity patterns. Images (A), (B), and (C) correspond to the simulation of the near-field fluorescence patterns generated with tilts of 0.0°, 2.1°, and 13.5°, respectively. The line cuts were performed in the direction of the polarization of the light at the positions indicated by the horizontal lines inserted into the left panels.

square of the electric field aligned with it, calculated using Bethe–Bouwkamp theory.[8] The results of such calculations for various tilts of the transition dipole moment are shown in Fig. 5 along with line cuts through the simulated intensity patterns. Comparison of line cuts from the experimental and calculated data such as those displayed in Figs. 4 and 5, respectively, reveal a near-field tip diameter of 72 nm and a z/a ratio of 0.9, where z is the tip-sample gap and a is the NSOM tip aperture radius. The measured fluorescence patterns shown in Figs. 4(A), 4(B), and 4(C) are best fit using transition dipole moment tilts (θ) of 0.0°, 2.1°, and 13.5°, respectively, which are displayed in Fig. 5.

Using this approach, the structure in DPPC monolayers transferred under conditions of low and high surface pressure are compared using data collected with the same near-field tip. Figure 6 illustrates the single molecule orientation distributions for TRITC–DHPE doped into DPPC monolayers at $\pi = 8$ and $\pi = 30$ mN/m. Approximately 60 molecules were analyzed under each film condition. Line cuts such as those shown in Fig. 4 were fit with a sum of two Gaussian curves from which the ratio of peak heights were extracted. As illustrated in Figs. 4 and 5, this ratio is very sensitive to the degree of tilt in the transition dipole moment. The analysis reveals average transition dipole tilt angles of 2.2° ($\sigma = 4.8°$) at low pressure and 2.4° ($\sigma = 5.0°$) at high pressure. Depending on the signal-to-noise of the particular feature, each of the measured tilt angles comprising the histogram are accurate within $\pm 0.5°$ to 1.0°.

The distributions are remarkably similar and both show the same preference in tilt direction. The uniformity in the tilt direction throughout the film is evidenced by the single peak in the tilt angle histograms. In fact, we find no statistical difference in the orientation of the probe molecule under the two film conditions studied, which will be evaluated further in the discussion section. At both surface pressures, we also find evidence for molecules tilted beyond the maximum tilt angle (16°) reported in Fig. 6. These molecules are tilted such that one lobe of the pattern is lost in the signal-to-noise and they appear as single lobed features in the data. These molecules are difficult to analyze accurately and were therefore not included in the histograms reported in Fig. 6. However, ~13% of the molecules in each film condition appear to have tilt angles greater than 16° which merits comment.

As mentioned earlier, the results from the simulated data

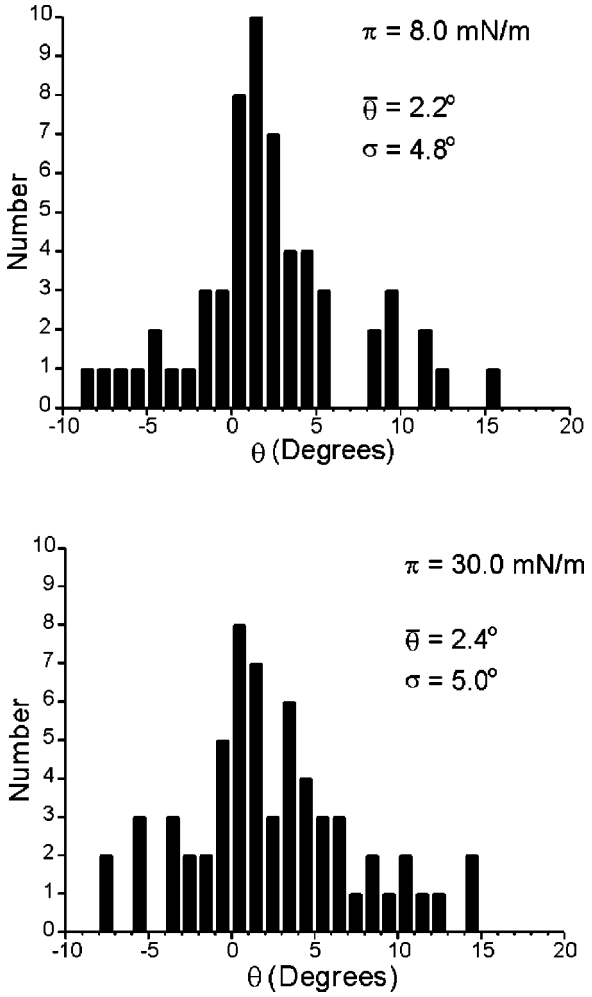

FIG. 6. Histograms of the measured transition dipole moment tilt for TRITC–DHPE in DPPC monolayers at surface pressures of $\pi = 8$ mN/m (top) and $\pi = 30$ mN/m (bottom). The distributions reflect 59 molecules (top) and 61 molecules (bottom) and only contain data from single molecule signals for which a dual lobed pattern was observed.

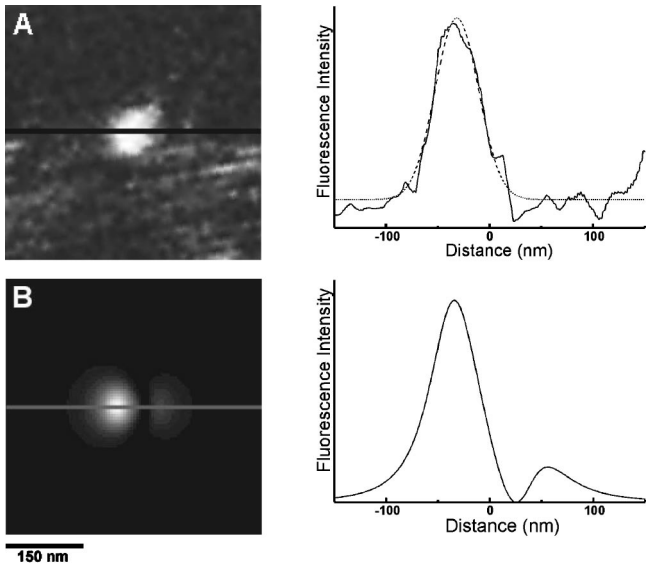

FIG. 7. A small population of probe molecules (~13%) are tilted beyond the point where dual-lobed fluorescent patterns, such as those observed in Fig. 4, are detected. These molecules give rise to near-field fluorescence features that appear sharper than that expected for the 72 nm diameter near-field aperture utilized in the imaging. (A) Near-field fluorescence signal (left) and line cut (right, solid line) of a representative molecule. The line cut is fit with a Gaussian (dashed line). (B) Simulated near-field fluorescence signal (left) and line cut (right) for a molecule tilted 20°. The FWHM of 54 nm for the more intense lobe of the calculated data is equal to that of the near-field fluorescence pattern shown in (A). The line cuts were performed in the direction of the polarization of the light at the positions indicated by the horizontal lines inserted into the left panels. Image (A) has been rotated for this alignment.

are best fit using a near-field tip diameter of 72 nm. However, single-lobed features in the data routinely exhibit a full-width-half-maximum (FWHM) that is significantly smaller than this aperture diameter. These results can be explained as molecules tilted beyond our ability to detect both lobes in the fluorescence pattern but not lying directly in the membrane plane where the FWHM would be near that of the tip aperture. In fact, analysis of the images reveals no convincing evidence for any molecules oriented such that their transition dipole moment lies in the plane of the film.

The fluorescence pattern of a representative single lobed emission feature is shown in Fig. 7(A) along with the corresponding line cut through the data. As the line cut illustrates, the FWHM of this feature is 54 nm which is much smaller than the 72 nm aperture used in the imaging. This can be compared with Fig. 7(B), showing the simulated fluorescence signal for a dipole tilted 20°, calculated using the tip aperture of 72 nm and z/a value of 0.9 found previously. The simulated signal clearly shows the presence of the second lobe of much reduced amplitude. This second lobe is hidden in the noise of the experimental data such that the fluorescence feature appears as a single lobe of higher than expected resolution. Without the second lobe, modeling of the tilt angle requires matching the peak shape from the data with the simulated signal. This is much less sensitive to the tilt angle which adds a significant increase in uncertainty for the reported angles. For molecules tilted beyond our ability to measure both lobes, the angle determination is only accurate to approximately $\pm 10°$.

DISCUSSION

The single molecule data displayed in Fig. 4 and analyzed in Fig. 5 clearly demonstrate the ability to characterize the molecular level structure in lipid membranes with NSOM. Distributions such as those shown in Fig. 6 not only reveal the average orientations but, more interestingly, the specific distribution of molecules that make up the ensemble average. This provides a detailed picture of the membrane organization that can easily be extended to more complicated studies on protein and peptide insertion into biological membranes. Moreover, as illustrated in Fig. 2, the simultaneous near-field topography measurements add an important dimension by providing a consistent and complementary view of sample properties that is particularly informative when combined with the near-field fluorescence measurements.[39,40,42]

Comparing the near-field force and fluorescence images shown in Figs. 2(A) and 2(B) confirms that the fluorescent probe molecule TRITC–DHPE partitions into the less or-

dered LE lipid phase, which is characterized by regions of reduced height in the force image and bright regions in the fluorescence image. As discussed earlier, reducing the probe concentration leads to the observation of single TRITC–DHPE molecules in the lipid film [Fig. 2(C)]. The individual single molecule signals are found to consist of various shapes which others have shown can be analyzed to extract the three-dimensional orientation of the probe in the sample.[7,8] For our particular system, this manifests itself as two-lobed fluorescent patterns in the near-field fluorescence image which indicates that the majority of the absorption transition dipole moments are orientated perpendicular to the plane of the membrane. This is illustrated in the schematic shown in Fig. 3 and shown in the experimental data displayed in Figs. 2(C) and 4.

Using a simplified model for the near-field aperture,[45,46] the fluorescent measurements can be modeled to extract the tilt angle of the individual probe molecules (Fig. 5).[7,8] Analysis of near-field fluorescence images of DPPC monolayers at low ($\pi = 8$ mN/m) and high ($\pi = 30$ mN/m) surface pressures yield the transition dipole moment tilt distributions shown in Fig. 6. The distribution in molecular orientations show remarkably narrow distributions for both film conditions. The small variance in the distributions reflect a high degree of homogeneity in the films and in the lipids surrounding the probe molecules, attesting to the quality of the lipid monolayers.

Somewhat surprisingly, we find no statistical difference in the tilt angles for probe molecules dispersed in DPPC monolayers at surface pressures of $\pi = 8$ mN/m and $\pi = 30$ mN/m. This, at first, is counterintuitive given the large structural changes known to accompany transitions from one lipid phase to another. For example, the 5 to 8 Å height changes in the near-field force images displayed in Figs. 2(B) and 2(D) are indicative of changes in the tilting of the lipids in going from the less ordered LE phase to the more structurally upright LC phase.[33,35,40,44] However, we find no statistical difference in the tilt angles for TRITC–DHPE molecules doped in the two film conditions.

There are several possible explanations for the insensitivity of the measured tilt angle to the surface pressure of the monolayer. It is possible that the TRITC–DHPE probe is insensitive to changes in the tilt of the surrounding lipid matrix because the fluorophore is located near the headgroup region of the monolayer.[51] Moreover, since the monolayers are transferred onto the mica surface in a headgroup down orientation, interactions with the surface may further decrease the probe sensitivity to tilt. However, preliminary single molecule measurements in our laboratory using a fluorescent probe in which the fluorophore is located in the tailgroup regions of the film indicates a similar insensitivity to surface pressure, suggesting that this is not the case.

Instead, our results agree with far-field studies on similar films deposited on an alkylated glass slide.[52] In this study, the fluorescent lipid analog NBD–PE was doped into monolayers of DPPC. This probe preferentially partitions into the less ordered lipid phase analogous to the TRITC–DHPE probe utilized in these studies. Using a polarized evanescent field to excite the NBD–PE probe, the average orientation was determined by analyzing the absorption dichroism as detected by the fluorescence emission. This study found that the NBD analog had an average tilt angle of 34.0° in DPPC films which changed little with surface pressure. This insensitivity to surface pressure was interpreted as arising from probe molecules staying trapped in small, less ordered lipid phases even as the pressure was increased.[52]

Our findings that the single molecule tilt distributions are the same for DPPC films at $\pi = 8$ mN/m and $\pi = 30$ mN/m tends to support this mechanism. This suggests that any changes taking place in the immediate surroundings of the probe molecule are not sufficiently large to dramatically affect the orientation of the probe molecule. However, recent far-field single molecule results from our laboratory indicate that the immediate freedom around the probe molecule is affected by increasing the film surface pressure.[47] This study found that the frequency of intensity fluctuations for the fluorescent lipid probe diIC_{18}, was intimately tied to the surface pressure of the lipid film. This was interpreted as reflecting a decrease in the tailgroup freedom of the film as the surface pressure increased. Taken together, these studies suggest that the environment around the probe molecule does change with surface pressure, but not enough to significantly affect the orientation of the molecule.

As discussed earlier, we find no evidence in either film condition for TRITC–DHPE probe molecules oriented with their dipole moments aligned in the plane of the film. However, we find that ~13% are oriented with tilt angles greater than 16° which is currently beyond our ability to observe the double-lobed fluorescence signals. These molecules appear as a very high resolution features since they are essentially only excited when located under one side of the near-field aperture.

Figure 7(A) displays a typical molecule that has a tilt angle beyond where we can detect the two-lobed structure. The matching simulated fluorescence signal shown in Fig. 7(B) indicates this particular transition dipole moment is tilted 20° with respect to the membrane normal. However, as mentioned earlier, the determination of tilt angles for these molecules is much less accurate since it is based on fitting the shape of the fluorescence signal. Whereas the tilt angle for a dual-lobed single molecule signal can be determined to be better than $\pm 1.0°$ depending on the signal-to-noise, for the single lobed features the tilt can only be determined to $\pm 10°$. For this reason, these molecules were excluded from the distributions shown in Fig. 6.

The ability to detect this minor, but significantly different population represents one of the key advantages of single molecule studies. The narrow tilt distributions presented in Fig. 6, measured using the dual-lobed fluorescence signals, suggest that the majority of the probe molecules insert into the membrane in well-defined positions with little tilt freedom. The observation of a second population tilted significantly beyond the mean value of 2.3° suggests another mechanism for probe insertion into DPPC monolayers. However, one trivial source of highly tilted molecules can arise from defects in the membrane structure. Examination of the near-field force images suggests that any defects in the membrane, if present, are small on the nanometer scale. This sug-

gests that membrane defects are not the dominant mechanism leading to the observed larger tilt angles. Therefore, this small population may represent a geometry in which the headgroup of the TRITC–DHPE probe molecule lies significantly beyond the lipid head-group plane. This would lead to a greater tilt in the long axis of the chromophore which has been suggested by previous far-field measurements on similar systems.[53,54]

With better signal-to-noise in the fluorescence signal and more control over the precise geometry of the near-field tip aperture, a larger range of single molecule tilt angles can be measured. For example, with the same tip aperture utilized here, calculations reveal an order of magnitude increase in the fluorescence signal is possible by simply reducing the tip-sample gap (z/a) from 0.90 to 0.27. This, however, neglects contributions from fluorescence quenching by the nearby metal coated tip which will tend to reduce the signal.[55–59] The calculations also indicate a difference in tilt sensitivity that is coupled with changes in the tip-sample gap. It may be possible, therefore, to both increase the signal and tune the sensitivity to the tilt angle by precisely controlling the geometry of the near-field tip. This has recently been demonstrated by van Hulst and co-workers.[7,60]

These researchers demonstrated the ability to precisely define the geometry of the near-field tip aperture by micromachining the tips using focused ion beam technology.[7,60] The resulting single molecule near-field fluorescence images exhibit patterns indicative of small z/a ranges.[7] At these reduced tip-sample gaps, calculations indicate that the dual-lobed single molecule signals are slightly less sensitive to tilt angle which means both lobes are observable at higher tilting angles than those shown here. This may enable, for instance, the accurate measurement of the highly tilted molecules found in this study. They also found a significant increase in the fluorescence signal with the micro-machined near-field tips.[7] This gain may also greatly improve the analysis of the highly tilted molecules, extending the range and utility of this technique.

CONCLUSIONS

Single molecule near-field fluorescence measurements are utilized to probe the molecular level structure in supported DPPC monolayers at low ($\pi = 8$ mN/m) and high ($\pi = 30$ mN/m) surface pressures. By analyzing the patterns observed in the fluorescence signal, the tilt angles for individual fluorescent TRITC–DHPE lipid analogs doped into the monolayers can be measured. Analysis of the fluorescence images reveal that the majority of the TRITC–DHPE probes insert in the film such that their absorption dipole moments are oriented approximately normal to the membrane surface. Histograms of the measured angles results in a mean tilt of 2.2° ($\sigma = 4.8°$) at low pressure and 2.4° ($\sigma = 5.0°$) for monolayers transferred at high pressure. We find no statistical difference between the two distributions. The insensitivity in tilt angle to surface pressure may reflect LE lipid phase domains remaining trapped in the film at elevated surface pressures.[52] We find no evidence for probe molecules oriented with their dipole moment parallel to the membrane surface, but ~13%, of the fluorescence signals originate from molecules tilted beyond 16°. This highly tilted population may reflect a second insertion geometry for TRITC–DHPE in the DPPC monolayers.[53,54]

These results illustrate how the unique properties of near-field microscopy can be utilized to probe the specific, molecular level structure in model lipid membranes. Extending these studies into other biologically relevant systems is straightforward and may provide a general and useful tool for the biological sciences. These measurements can provide new clues into specific structure-function relationships, free from the ensemble averaging encountered with bulk techniques.

ACKNOWLEDGMENTS

The authors wish to thank Professor Brian Laird and Jess Sturgeon for the helpful discussions. We gratefully acknowledge the support of NSF (CHE-9612730) and the Searle Scholars Program/The Chicago Community Trust.

[1] E. Betzig, J. K. Trautman, T. D. Harris, J. S. Weiner, and R. L. Kostelak, Science **251**, 1468 (1991).
[2] *Scanning Near-Field Optical Microscopy (SNOM)*, edited by D. W. Pohl (Academic, London, 1991), Vol. 12.
[3] Special Issue on Near-Field Optics, J. Microsc. **194**, 1 (1999).
[4] M. A. Paesler and P. J. Moyer, *Near-Field Optics: Theory, Instrumentation, and Applications* (Wiley, New York, 1996).
[5] D. A. Vanden Bout, J. Kerimo, D. A. Higgins, and P. F. Barbara, Acc. Chem. Res. **30**, 204 (1997).
[6] R. C. Dunn, Chem. Rev. **99**, 2891 (1999).
[7] J. A. Veerman, M. F. Garcia-Parajo, L. Kuipers, and N. F. van Hulst, J. Microsc. **194**, 477 (1999).
[8] E. Betzig and R. J. Chichester, Science **262**, 1422 (1993).
[9] D. Zhang, J. Gutow, and K. B. Eisenthal, J. Phys. Chem. **98**, 13729 (1994).
[10] J. D. LeGrange, H. E. Reigker, W. P. Zurawsky, and S. F. Scarlata, J. Chem. Phys. **90**, 3838 (1989).
[11] N. Kimura *et al.*, Chem. Phys. Lipids **57**, 39 (1991).
[12] T. Enderle, A. J. Meixner, and I. Zschokke-Granacher, J. Chem. Phys. **101**, 4365 (1994).
[13] P. L. Edmiston, J. E. Lee, L. L. Wood, and S. S. Saavedra, J. Phys. Chem. **100**, 775 (1996).
[14] S. B. Dierker, C. A. Murray, J. D. Legrange, and N. E. Schlotter, Chem. Phys. Lett. **137**, 453 (1987).
[15] J. Jansy and J. Sepiol, Chem. Phys. Lett. **273**, 439 (1997).
[16] J. Sepiol, J. Jansy, J. Keller, and U. P. Wild, Chem. Phys. Lett. **273**, 444 (1997).
[17] A. P. Bartko and R. M. Dickson, J. Phys. Chem. B **103**, 3053 (1999).
[18] R. M. Dickson, D. J. Norris, and W. E. Moerner, Phys. Rev. Lett. **81**, 5322 (1998).
[19] X. S. Xie and J. K. Trautman, Annu. Rev. Phys. Chem. **49**, 441 (1998).
[20] C. E. Talley, G. Cooksey, and R. C. Dunn, Appl. Phys. Lett. **69**, 3809 (1996).
[21] T. Enderle *et al.*, Proc. Natl. Acad. Sci. USA **94**, 520 (1997).
[22] T. Enderle, T. Ha, D. S. Chemla, and S. Weiss, Ultramicroscopy **71**, 303 (1998).
[23] N. F. van Hulst, M. F. Garcia-Parajo, M. H. P. Moers, J.-A. Veerman, and A. G. T. Ruiter, J. Struct. Biol. **119**, 222 (1997).
[24] R. C. Dunn, G. H. Holtom, L. Mets, and X. S. Xie, J. Phys. Chem. **98**, 3094 (1994).
[25] J. Hwang, L. A. Gheber, L. Margolis, and M. Edidin, Biophys. J. **74**, 2184 (1998).
[26] R. B. Gennis, *Biomembranes: Molecular Structure and Function* (Springer-Verlag, New York, 1989).
[27] H. M. McConnell, Annu. Rev. Phys. Chem. **42**, 171 (1991).
[28] H. Möhwald, Annu. Rev. Phys. Chem. **41**, 441 (1990).
[29] G. L. Gaines, *Insoluble Monolayers at Gas Liquid Interfaces* (Interscience, New York, 1966).
[30] M. M. Lipp, K. Y. C. Lee, A. Waring, and J. A. Zasadzinski, Biophys. J. **72**, 2783 (1997).

[31] J. Hwang, L. K. Tamm, C. Bohm, T. Ramalingam, E. Betzig, and M. Edidin, Science **270**, 610 (1995).
[32] C. M. Knobler, Science **249**, 870 (1990).
[33] L. F. Chi, M. Anders, H. Fuchs, R. R. Johnston, and H. Ringsdorf, Science **259**, 213 (1993).
[34] L. F. Chi, H. Fuchs, R. R. Johnston, and H. Ringsdorf, Thin Solid Films **242**, 151 (1994).
[35] J. M. Mikrut, P. Dutta, J. B. Ketterson, and R. C. MacDonald, Phys. Rev. B **48**, 14479 (1993).
[36] X. M. Yang, D. Xiao, S. J. Xiao, and Y. Wei, Appl. Phys. A: Solids Surf. **A59**, 139 (1994).
[37] X. M. Yang, D. Xiao, Z. H. Lu, and Y. Wei, Appl. Surf. Sci. **90**, 175 (1995).
[38] P. Yeagle, *The Structure of Biological Membranes* (CRC Press, Boca Raton, 1992).
[39] C. W. Hollars and R. C. Dunn, J. Phys. Chem. B **101**, 6313 (1997).
[40] C. W. Hollars and R. C. Dunn, Biophys. J. **75**, 342 (1998).
[41] L. K. Tamm *et al.*, Thin Solid Films **284–285**, 813 (1996).
[42] M. H. P. Moers, H. E. Gaub, and N. F. van Hulst, Langmuir **10**, 2774 (1994).
[43] H. Shiku and R. C. Dunn, J. Microsc. **194**, 461 (1999).
[44] H. Shiku and R. C. Dunn, J. Phys. Chem. B **102**, 3791 (1998).
[45] H. A. Bethe, Phys. Rev. **66**, 163 (1944).
[46] C. J. Bouwkamp, Philips Res. Rep. **5**, 321 (1950).
[47] C. E. Talley and R. C. Dunn, J. Phys. Chem. B **103**, 10214 (1999).
[48] C. Talley, M. A. Lee, and R. C. Dunn, Appl. Phys. Lett. **72**, 2954 (1998).
[49] C. W. Hollars and R. C. Dunn, Rev. Sci. Instrum. **69**, 1747 (1996).
[50] D. A. Cadenhead, F. Müller-Landau, and B. M. J. Kellner, in *Ordering in Two Dimensions*, edited by S. K. Sinha (Elsevier, Amsterdam, 1980), pp. 73–81.
[51] X. Zhai and J. M. Kleijn, Biophys. J. **72**, 2651 (1997).
[52] N. L. Thompson, H. M. McConnell, and T. P. Burghardt, Biophys. J. **46**, 739 (1984).
[53] L. B.-Å. Johansson and V. Ö. Sundstrom, Chem. Phys. Lett. **167**, 383 (1990).
[54] T. Schmidt, G. J. Schutz, W. Baumgartner, H. J. Gruber, and H. Schindler, J. Phys. Chem. **99**, 17662 (1995).
[55] R. X. Bian, R. C. Dunn, X. S. Xie, and P. T. Leung, Phys. Rev. Lett. **75**, 4772 (1995).
[56] R. R. Chance, A. Prock, and R. Silbey, Adv. Chem. Phys. **37**, 1–65 (1978).
[57] X. S. Xie and R. C. Dunn, Science **265**, 361 (1994).
[58] W. P. Ambrose, P. M. Goodwin, J. C. Martin, and R. A. Keller, Science **265**, 364 (1994).
[59] J. K. Trautman and J. J. Macklin, Chem. Rev. **205**, 221 (1996).
[60] J. A. Veerman, A. M. Otter, L. Kuipers, and N. F. van Hulst, Appl. Phys. Lett. **72**, 3115 (1998).